Numerical study of the influence of solid polarization on electrophoresis at finite Debye thickness

Somnath Bhattacharyya* and Simanta De†
Department of Mathematics, Indian Institute of Technology Kharagpur, Kharagpur-721302, India
(Received 18 May 2015; published 24 September 2015)

The influence of solid polarization on the electrophoresis of a uniformly charged dielectric particle for finite values of the particle-to-fluid dielectric permittivity ratio is analyzed quantitatively without imposing the thin Debye length or weak-field assumption. Present analysis is based on the computation of the coupled Poisson-Nernst-Planck and Stokes equations in the fluid domain along with the Laplace equation within the solid. The electrophoretic velocity is determined through the balance of forces acting on the particle. The solid polarization of the charged particle produces a reduction on its electrophoretic velocity compared to a nonpolarizable particle of the same surface charge density. In accordance with the existing thin-layer analysis, our computed results for thin Debye layer shows that the solid polarization is important only when the applied electric field is strong. When the Debye length is in the order of the particle size, the electrophoretic velocity decreases with the rise of the particle permittivity and attains a saturation limit at large values of the permittivity. Our computed solution for electrophoretic velocity is in agreement with the existing asymptotic analyses based on a thin Debye layer for limiting cases.

DOI: 10.1103/PhysRevE.92.032309 PACS number(s): 82.45.Tv, 82.39.Wj, 87.15.Tt, 77.84.−s

I. INTRODUCTION

The surface charge density (or surface potential) of a nonpolarizable (perfect dielectric) particle can be considered to be independent of the applied electric field. However, the solid polarization of a dielectric (polarizable) particle due to an imposed electric field induces a nonuniform surface potential. The solid polarization is characterized by the ratio of the solid-to-liquid dielectric permittivity ratio. O'Brien and White [1] demonstrated through the weak-field analysis that the electrophoretic mobility does not depend on the particle dielectric constant. However, the thin-layer analysis of Yossifon *et al.* [2] shows that the solid polarization can have a significant role when the solid-to-electrolyte permittivity ratio is large. The asymptotic analysis of Schnitzer and Yariv [3], and the references there-in demonstrate that the solid polarization affects the leading-order electrokinetic transport when the applied electric field is strong enough to create a potential drop across the Debye layer in the order of the thermal potential. Their asymptotic analysis revels that the solid polarization affects the electrophoretic velocity of the particle even for small values of solid-to-liquid permittivity ratios under a strong external electric field.

The electroosmotic flow around a conducting surface is referred to as the induced-charge electroosmosis (ICEO). The micro-PIV measurement (Canpolat *et al.* [4]) of ICEO around a metallic rod shows that the flow is quadrupolar and has a much stronger fluid motion than the conventional electroosmotic flow (EOF) under a specified electric field. A detailed description of the ICEO near a ideally polarizable particle is made by Squires and Bazant [5]. The solid polarization of a conducting particle of symmetric geometry and homogeneous properties have no effect on its transportation. However, the polarization could cause the asymmetric particle to move and is termed as the induced-charge electrophoresis (ICEP). The mathematical models for ICEP of conducting particle was introduced by Yariv [6] and Squires and Bazant [7]. The induced-charge electrophoresis of an uncharged conducting symmetric particle such as a cylinder or sphere in the vicinity of a nonpolarizable uncharged surface has been analyzed under a thin Debye length by Zhao and Bau [8], Yariv [9], and Hamed and Yariv [10].

The slip-flow model, which is based on the induced ζ potential and the Smoluchowski slip velocity at the edge of the Debye layer, is inapplicable when the Debye length is comparable with the particle size. The ICEO around a conducting surface for moderate range of Debye layer was considered by Yariv and Miloh [11]. Their analysis was based on the weak-field approximation. The electrokinetic flow about an ideally polarizable spherical particle with thick Debye layer was analyzed by Abu Hamed and Yariv [12] using an inner-outer asymptotic expansion under a weak-field assumption. Analysis of ICEO about a metallic cylinder based on direct numerical simulations of the coupled Poisson-Nernst-Planck and Navier-Stokes equations is made recently by Davidson *et al.* [13]. Their results show that induced-charge electrokinetic can be chaotic at a high applied electric field.

Most solids that are commonly used in electrokinetics may not be perfectly conducting (or ideally polarizable). Schnitzer and Yariv [14] have pointed-out certain characteristic differences of the electrokinetic flow about a perfectly conducting particle from a dielectric particle. For a dielectric solid, the electric potential is nonuniform, which must be solved inside the particle and then matched to that in the liquid. Under a small ζ potential assumption, Yossifon *et al.* [2] studied the ICEO about a dielectric particle of large dielectric constant and demonstrated a technique to determine the induced ζ potential in a thin Debye layer limit, which relates the electric potentials within the dielectric solid and the bulk electroneutral solution. Subsequently, Yariv and Davis [15] considered the electroosmotic flows over a highly polarizable surface under the thin Debye layer assumption without imposing a condition of small ζ potential. The asymptotic analysis of Yariv and Davis [15] shows that the solid polarization affects the

*somnath@maths.iitkgp.ernet.in
†simanta.de@gmail.com

electrokinetic processes even for the thin Debye layer case when the dielectric ratio between the solid-to-fluid is large. The study of Schnitzer and Yariv [14] on the electroosmotic flow about a dielectric surface of zero surface charge shows that the induced EOF undergoes a transition from a quadratic variation with the imposed electric field for low to moderate range of imposed field to a linear variation when a strong electric field is considered.

In this paper, we consider the electrophoresis of a dielectric charged particle based on the first principle of electrokinetics. The coupled set of equations governing the electrokinetics is solved numerically without making any simplifications based on the thin double layer or weak applied electric-field assumptions. Thus, the present study takes into account the surface conduction and solid polarization automatically. Under the thin-double-layer limit, the electric field lines can be assumed to be tangential to the surface. However, for a highly charged particle, surface conduction can be appreciable and its effects on electrokinetics must be taken into account. The study on electrophoresis of an ideally polarizable particle by Figliuzzi *et al.* [16] shows that the surface conduction significantly decreases the electrophoretic mobility when the particle surface potential and applied electric field are strong. The parameter, Dukhin number expresses the importance of the surface conduction. An account of previous studies dealing with the role of surface conduction on electrophoresis is provided by Schnitzer and Yariv [17]. There they have analyzed the electrokinetic flow about a highly charged surface in the limit of a thin double layer but relaxing the weak applied field limitation underlying the classical work of O'Brien [18] and O'Brien and Hunter [19]. A weak-field analysis appearing in Schnitzer and Yariv [17] shows that the solid polarization for the thin-double-layer case does not affect the leading order transport properties. Subsequently, Schnitzer *et al.* [20] extended the weak-field approximation of Schnitzer and Yariv [17] to obtain a nonlinear velocity correction proportional to the field cubed. Recently, Schnitzer and Yariv [21] analyzed the general problem of electrophoresis of the thin-double-layer limit, as considered by Schnitzer and Yariv [17], and obtained a nonlinear solution for the electrophoretic velocity for small but finite Dukhin number.

The present work is based on the computation of the governing Poisson-Nernst-Planck and Stokes equations. The agreement of our computed results with the existing asymptotic analysis is encouraging. In practical context, the bioparticles have moderate range of particle-to-electrolyte permittivity ratio and the thickness of the double layer may appear to be in the order of the particle size. We have analyzed the electrophoresis for finite Debye length and moderate range of the applied electric field for a wide range of the particle-to-electrolyte dielectric permittivity ratio. Our results show that the effect of solid polarization is significant when the Debye layer thickness is comparable with the particle size.

II. MATHEMATICAL MODEL

A dielectric spherical particle of radius a with uniform surface charge density σ and dielectric permittivity ε_p is submerged in an electrolyte of permittivity ε_e. A uniform

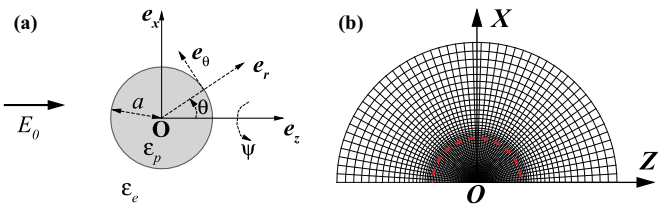

FIG. 1. (Color online) Schematic description of the geometry and the spherical coordinate system is shown in panel (a). Grid distribution inside and around the solid sphere is shown in panel (b). The dashed red line represents the surface of the particle. The potential field is computed within the particle.

electrical field E_0 is imposed far from the particle. As a result of the electrostatic force, the particle migrates with a velocity U_E^* relative to the otherwise quiescent electrolyte. The migration speed U_E^* is unknown *a priori*. Our intention is to determine the electrophoretic velocity U_E^* of the particle. This problem is equivalent to that of a stationary sphere experiencing an incoming flow at a uniform velocity of $-U_E^*$ far from the particle surface in a frame of reference fixed at the center of the particle. We define the spherical coordinate (r,θ,ψ) system with its origin fixed at the center of the particle [Fig. 1(a)] and axial direction is along the imposed field E_0. The equations governing this electrokinetic phenomena are the Stokes equation with electric body force term for fluid flow and the Nernst-Planck equations for ion transport. The electric field in the electrolyte is governed by the Poisson equation, whereas the electric potential inside the particle satisfies the Laplace equation. Following Saville [22], we scale the dimensional variables as follows: the length scale as the radius of the sphere a, the potential scale is $\phi_0 = k_B T/\mathcal{Z}e$, $U_0 = \varepsilon_e \phi_0^2/a\mu$ is the velocity scale, $\varepsilon_e\phi_0^2/a^2$ is the pressure scale, and the bulk ionic number n_0 is the scale for ionic concentration. The dimensionless Stokes equation for the incompressible Newtonian fluid is

$$\nabla p - \nabla^2 \boldsymbol{u} + \frac{(\kappa a)^2}{2}\rho_e \nabla\phi = 0, \tag{1}$$

$$\nabla \cdot \boldsymbol{u} = 0, \tag{2}$$

where $\boldsymbol{u}$ is velocity vector, p is pressure, and $\rho_e = (n_1 - n_2)$ is the charge density with n_i as the ionic concentration of ith ionic species with valence z_i. Since the present model is based on Nernst-Planck equations it has the flexibility to handle multivalent ions. For simplicity, we have considered symmetric z-z electrolyte with valance $z_i = \pm\mathcal{Z}$ for $i = 1,2$, respectively. Here ϕ and ϕ_p are denoted, respectively, the potential within the liquid or the particle. Here e is the elementary electric charge, k_B is the Boltzmann constant, T is the absolute temperature, and $\kappa = \sqrt{2\mathcal{Z}en_0/\varepsilon_e\phi_0}$ is the inverse of EDL thickness.

The nondimensional form of the Nernst-Planck equation governing the transport of the ith ionic species is

$$Pe(\boldsymbol{u}\cdot\nabla n_i) = \nabla^2 n_i \pm \nabla\cdot(n_i\nabla\phi). \tag{3}$$

For the sake of simplicity the diffusivity of the ions are considered to be equal and is equal to D. The nondimensional parameters governing the electrophoresis are $\mathrm{Pe} = \varepsilon_e\phi_0^2/\mu D$,

which provides the relative importance of electroconvection to electromigration (Khair and Squires [23]), the Debye-Huckel parameter κa, particle-to-electrolyte dielectric permittivity ratio $\varepsilon_r = \varepsilon_p/\varepsilon_e$, scaled surface charge density σ and the scaled electric field $\beta = E_0 a/\phi_0$. The uniform surface charge density is scaled by $\varepsilon_e \kappa \phi_0$. The ρ and μ are the density and the viscosity of the medium, respectively. The electric potential in the liquid satisfies the Poisson equation,

$$\nabla^2 \phi = -\frac{(\kappa a)^2}{2}\rho_e. \tag{4}$$

The electric potential inside the particle obeys the Laplace equation as the net charge density is zero within the particle,

$$\nabla^2 \phi_p = 0. \tag{5}$$

A nonslip boundary condition and no-normal flux of ions are imposed on the surface of the particle ($r = 1$),

$$\boldsymbol{u} = \boldsymbol{0},\ (\nabla n_i \pm n_i \nabla \phi)\cdot \boldsymbol{e_r} = 0. \tag{6}$$

The jump in the electric displacement on the surface of the particle ($r = 1$) is related to the surface charge density as

$$\frac{\partial \phi}{\partial r} - \varepsilon_r \frac{\partial \phi_p}{\partial r} = -(\kappa a)\sigma,\ \phi_p = \phi; \tag{7}$$

the later condition is governed by the electric-potential continuity. Far from the particle ($r \to \infty$),

$$\boldsymbol{u} = -U_E \boldsymbol{e_z},\ \phi = -\beta r\cos\theta,\ n_i = 1. \tag{8}$$

In the far field, the gradient of the electric potential must approach the applied electric field. Here $\boldsymbol{e_r}$ and $\boldsymbol{e_z}$ are the unit vectors along the radial and axial direction, respectively. A symmetry condition is imposed along the axis of symmetry; i.e., $\theta = 0,\pi$. In this study we have restricted our attention for finite values of ε_r and κa.

The problem can be considered to be axisymmetric and steady. However, we adopt a time-marching procedure to obtain the steady-state solution with the initial condition being governed by the equilibrium condition with particle initially at rest. The electrophoretic velocity of the particle (U_E) is obtained by solving iteratively the balance of drag and electric forces experienced by the particle. The iteration process starts with an initial assumption for electrophoretic velocity based on the Henry mobility [24]. The drag and electric forces are obtained by computing the governing equations using the approximate value of the electrophoretic velocity. Iteration process continues till the balance of forces is established.

The forces experienced by the particle are the electric force and drag force. The axisymmetric nature of our problem suggests that only the z component of these forces need to be considered. The electrostatic and hydrodynamic forces along the flow direction can be calculated by integrating the Maxwell stress tensor $\boldsymbol{\sigma^E}$ and hydrodynamic stress tensor $\boldsymbol{\sigma^H}$, respectively, on the surface of the particle and are given by

$$F_E^* = \iint_S (\boldsymbol{\sigma^E}\cdot \boldsymbol{e_r})\cdot \boldsymbol{e_z}\, dS, \tag{9}$$

$$F_D^* = \iint_S (\boldsymbol{\sigma^H}\cdot \boldsymbol{e_r})\cdot \boldsymbol{e_z}\, dS, \tag{10}$$

where $\boldsymbol{\sigma^E} = \varepsilon_e[\boldsymbol{EE} - (1/2)E^2\boldsymbol{I}]$ and $\boldsymbol{\sigma^H} = -p\boldsymbol{I} + \mu[\nabla \boldsymbol{u} + (\nabla \boldsymbol{u})^T]$. Here $\boldsymbol{E} = -\nabla\phi$, $E^2 = \boldsymbol{E}\cdot\boldsymbol{E}$, $\boldsymbol{EE}$ denotes the vector direct product and $\boldsymbol{I}$ is the unit tensor. The variables with an asterisks denote dimensional quantities:

$$F_E = -\iint_S \left[\frac{\partial \phi}{\partial r}\frac{\partial \phi}{\partial z} - \frac{1}{2}\left\{\left(\frac{\partial \phi}{\partial r}\right)^2 + \left(\frac{1}{r}\frac{\partial \phi}{\partial \theta}\right)^2\right\}\cos\theta\right] dS, \tag{11}$$

$$F_D = -\iint_S \left[p\cos\theta + \sin\theta \frac{\partial u}{\partial r}\right] dS. \tag{12}$$

The forces F_E and F_D are scaled by $\varepsilon_e \phi_0^2$. Here u is the cross radial velocity component.

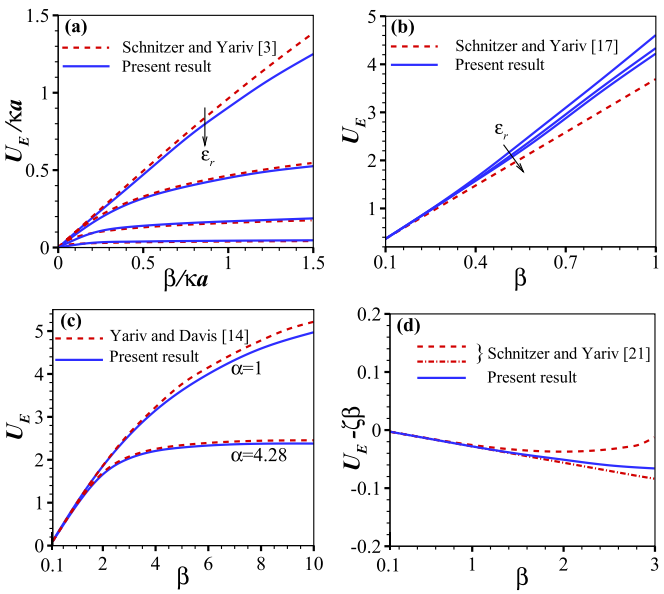

FIG. 2. (Color online) Comparison of our computed results for electrophoretic velocity as a function of the imposed electric field for large κa with the corresponding asymptotic models. Comparison with Schnitzer and Yariv [3] for different values of the permittivity ratio ε_r(=1, 10, 50, 300) with $\sigma = 1.04$ and $\kappa a = 70$ is shown in panel (a). Here, variables are rescaled by considering Debye length (κ^{-1}) as the length scale. Comparison with Schnitzer and Yariv [17] and Schnitzer *et al.* [20] for lower range of $\beta(\ll 1)$ when $\sigma = 20.03$, $\kappa a = 40.2$, and $\varepsilon_r = 1, 10, 300$ and comparison with Yariv and Davis [15] for different choice of $\alpha = \varepsilon_r/\kappa a = 1$ and 4.28 with $\sigma = 1.04$ and $\kappa a = 70$ are shown in panels (b) and (c), respectively. Variation of nonlinear velocity correction ($U_E - \zeta\beta$) with β when $\sigma = 1.04\,\kappa a = 50$, $\varepsilon_r = 300$, and Pe = 0.1, which corresponds to Du = 0.025 in panel (d). Here solid blue lines represent our computed results and dashed red lines corresponds to asymptotic solutions.

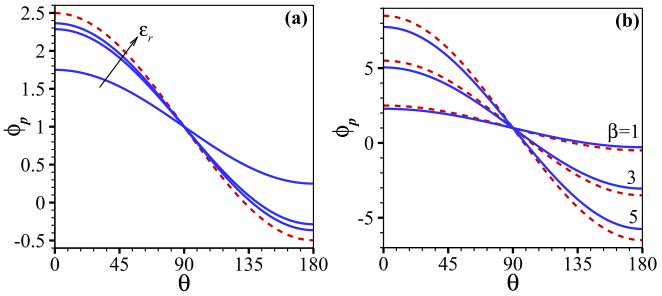

FIG. 3. (Color online) Variation of surface potential ϕ_p on the surface of the dielectric particle when $\kappa a = 50$, $\sigma = 1.04$ (a) for different $\varepsilon_r(=1, 50, 300)$ with $\beta = 1$; (b) for different $\beta(=1, 3, 5)$ when $\varepsilon_r = 50$. The dashed line corresponds to Squires and Bazant [5] for a perfectly polarizable particle.

III. NUMERICAL METHODS

The governing equations under the axisymmetric assumption are solved in a coupled manner through a control volume approach over a staggered grid arrangement. The discretized form of the governing equations is obtained by integrating the governing equations over each control volume. Different control volumes are used to integrate different equations.

The discretized equations are solved through the pressure correction based iterative SIMPLE (semi-implicit method for pressure-linked equations) algorithm. This procedure is based on a cyclic guess-and-correct operation to solve the governing equations. The pressure link between the continuity and momentum equations are accomplished by transforming the discretized continuity equation into a Poisson equation for pressure correction. This Poisson equation implements a pressure correction for a divergent velocity field. At each iteration the equations for electric field, i.e., Eqs. (4) and (5) are computed to obtain the potential field. Equations (4) and (5) are computed through the successive-over-relaxation (SOR) technique.

A time-dependent numerical solution is achieved by advancing the variables through a sequence of short time steps. We start the motion from the initial stationary condition and achieve a steady-state after a large time step for which the variables become independent of time. At the initial stage of motion, the time step is taken to be 0.001, which is subsequently increased to 0.005 after the transient state.

The variables near the surface of the rigid sphere varies more rapidly than elsewhere. In order to account for this fast change, we considered a nonuniform grid distribution along the r direction; however, a uniform grid is considered along the θ direction [Fig. 1(b)]. We adopt a finer grid distribution around the solid sphere. Grid size in the radial direction is then increased in an arithmetic progression as we move away from the sphere. We made a grid independency study by considering three sets of nonuniform grid points, namely 150×300, 150×350, and 150×400, with first and second number being the total number of grid points in θ and r directions, respectively. The optimal grid size is found to be 150×350, where the nonuniform radial grid size varies between 0.01 to 0.1 and a uniform grid is considered along the cross-radial direction. For the sake of brevity the grid independency test is not shown here. We have compared our computed results with the asymptotic models and found them in good agreement. A detailed discussion is made in the following section. Our computed solution for electrophoretic velocity of a nonpolarizable particle compares well with the velocity based on Henry's formula [24] for lower range of applied field. However, our computed solutions underpredicts the results based on the Henry's formula when applied field is strong.

IV. RESULTS AND DISCUSSION

We have compared our computed solutions with the solutions based on asymptotic methods for thin Debye length as obtained by several authors. The asymptotic solution as obtained by Schnitzer and Yariv [3] under strong-field condition for arbitrary values of ε_r is compared Fig. 2(a). We have considered $\kappa a = 70$ for moderate range of applied electric field when native surface charge density $\sigma = 1.04$, which corresponds to $\zeta = 1$ based on the relation $\sigma = 2\sinh(\zeta/2)$. In order to make the comparison, we have rescaled the velocity and electric field with the Debye length (κ^{-1}) as the length scale. A good agreement between the computed result and the asymptotic solution is evident for higher values of the dielectric permittivity ratio. However, a slight discrepancy between the computed solution and asymptotic result is evident at $\varepsilon_r = 1$ for large values of the imposed field. This may be due to the double-layer polarization (DLP) effect. In Fig. 2(b), we present a comparison of the electrophoretic velocity with the analytical formula (9.20) of Schnitzer and Yariv [17] for a highly charged dielectric particle with thin Debye layer under the weak applied field condition. The parameter values as considered by them

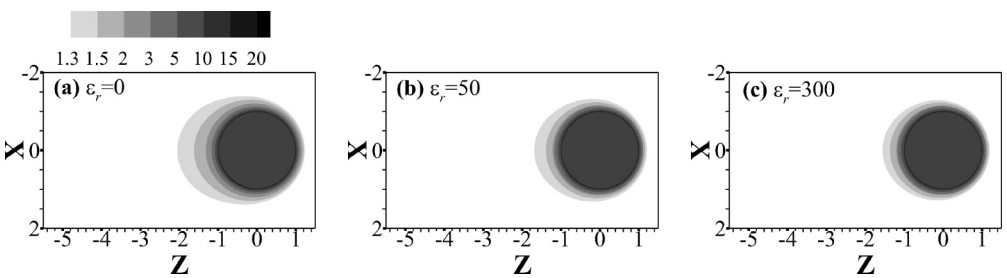

FIG. 4. Distribution of counterions around the particle for different values of its electric permittivity when $\sigma = 21.29$, $\kappa a = 5$, $\beta = 1$ for $\varepsilon_r = 0$, 50, and 300.

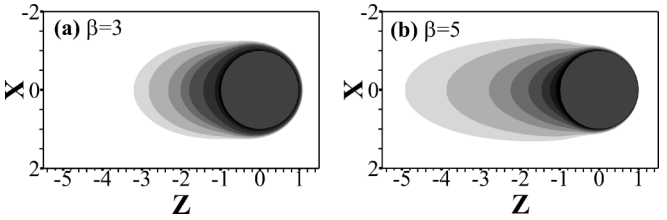

FIG. 5. Distribution of counterions around the particle for different values of nondimensional applied electric field β when $\sigma = 21.29$, $\kappa a = 5$, $\varepsilon_r = 50$ for $\beta = 3$ and 5. Contour levels are the same as described in the caption of Fig. 4.

suggest that $\kappa a = 40$ and $\zeta = 6$. We consider the permittivity ratio $\varepsilon_r = 1, 10, 300$. Our computed results agree well with the results obtained by Schnitzer and Yariv [17] for lower range of the imposed field. We made a comparison of our computed results with the asymptotic solution of Yariv and Davis [15] under a thin Debye layer assumption in Fig. 2(c). They estimated the electrophoretic velocity of a highly polarizable particle as a function of the polarization parameter $\alpha = \varepsilon_r/(\kappa a)$. We present results for different choice of ε_r and κa so as to have a constant value of α. We find that at large values of κa and ε_r our computed results is in agreement with those of Yariv and Davis [15]. This agreement is excellent for higher ε_r, i.e., $\varepsilon_r = 300$. In Fig. 2(d) the difference between the computed electrophoretic velocity from the linear Smoluchowski formula (i.e., $\beta\zeta$) as a function of the applied electric field is compared with the asymptotic solution Eqs. (67) and (69) of Schnitzer and Yariv [21] when the Dukhin number is small and Debye length is thin. We have considered $\kappa a = 50$, $\sigma = 1.04$, $\varepsilon_r = 300$, with diffusivity $D = 6.68\varepsilon_e$, which corresponds to Pe $= 0.1$ and Dukhin number Du $= 0.025$. Our computed results for $\kappa a = 50$ is in agreement with the asymptotic solution for low to moderate range of the imposedxbrk field.

Distribution of the surface potential along the outer surface of the particle is depicted in Figs. 3(a) and 3(b) for large values of κa (thin Debye layer) for different values of ε_r and β when the surface charge density is $\sigma = 1.04$. Under the influence of the imposed electric field the ions of opposite polarity moves along the direction of the electric field. Due to the nonpenetration condition on the solid surface, the positive ions accumulate on the side facing the electric field and negative ions cluster around the opposite face of the solid. This ionic cloud attracts image charges within the dielectric sphere. Thus,

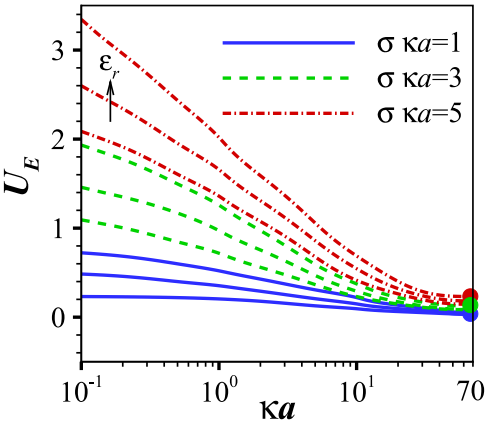

FIG. 7. (Color online) Variation of electrophoretic velocity with κa for different $\sigma\kappa a$(=1,3,5) and ε_r(=0.01,10,300) when $\beta = 1$. Symbols corresponds to velocity based on Henry function [24].

the Debye layer enveloping the dielectric particle is different from the Debye layer, which occurs around a nonpolarizable particle. The magnitude of the surface potential increases with the increase of the dielectric permittivity. This increment in magnitude with the increase of ε_r occurs at a faster rate for medium range of ε_r. At large ε_r, the induced potential approaches the value corresponding to an infinitely polarizable particle. The surface potential of an infinitely polarizable particle ($\varepsilon_r \to \infty$) under a thin Debye layer condition was given by Squires and Bazant [5] as $\phi_s = (3/2)\beta\cos\theta$. We find that as ε_r becomes large, the induced surface potential approaches the above analytic solution. Figure 3(b) shows the distribution of surface potential at different values of the imposed electric field. In Figs. 3(a) and 3(b) the dashed lines correspond to the analytic solution obtained by linear super position of $(3/2)\beta\cos\theta$ with the native surface potential ($\zeta = 1$) of the particle under a thin Debye layer assumption. Variation in the imposed electric field produces a large change in the induced electric potential. We have shown later that the strong dielectric polarization of the particle surface at high imposed field creates a large deviation of its electrophoresis from a nonpolarizable particle.

The motion of the particle creates a deformation of the electric double layer that is enveloping the particle, which in turn leads to a retardation effect on the electrophoresis. This phenomena is referred as the DLP and it is important when the Debye length is in the order of the particle size. The distribution

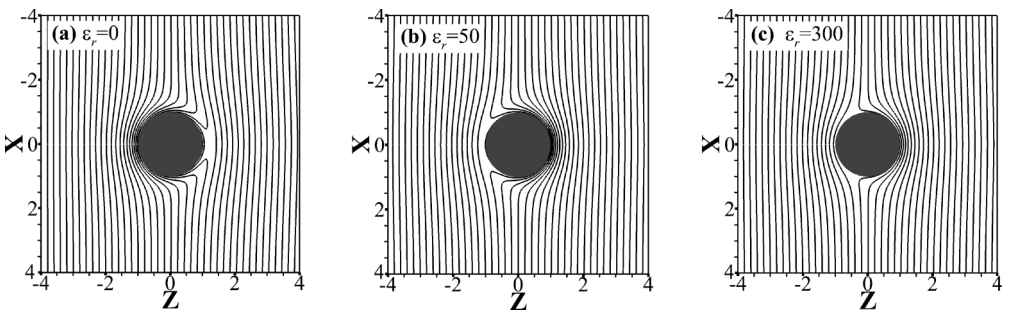

FIG. 6. Electric potential lines around dielectric particle for different ε_r when $\kappa a = 5$, $\beta = 1$, and $\sigma = 5.21$ for $\varepsilon_r = 0$, 50, and 300.

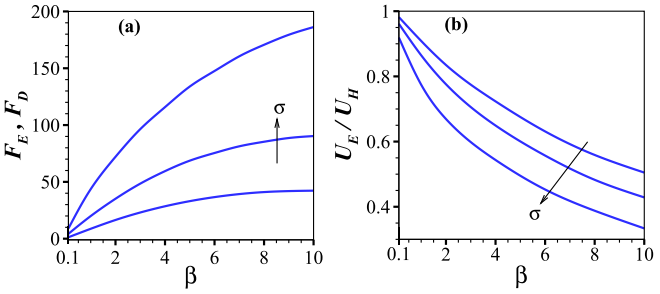

FIG. 8. (Color online) Variation of (a) hydrodynamic and electric forces; (b) ratio of electrophoretic velocity between a polarizable particle and nonpolarizable particle with applied electric filed β for different σ(=0.5, 1.04, 4.26), where $\kappa a = 50$, $\varepsilon_r = 50$.

of counterions near the particle for moderate value of the EDL thickness is illustrated in Figs. 4(a)–4(c) for different values of dielectric permittivity ratio. The deformation of the ion cloud near the particle is evident from the figure. The deformation of Debye layer and DLP is high for a nonpolarizable particle ($\varepsilon_r = 0$). A strong plume of counterions in downstream shows that the electric field generated due to the ion transport is opposite to the direction of the applied electric field. This DLP effect results in a net dipole moment that is antiparallel to the applied field. The impact of DLP accentuates when the Debye layer is in the order of the particle radius, i.e., $\kappa a \sim O(1)$ [25], and it reduces as the electric permittivity of the particle is raised. The deformation of double layer enhances as the imposed field grows [Figs. 5(a) and 5(b)]. It is evident from Figs. 4(b), 5(a), and 5(b) that the plume of counterions extends with the rise of electric field.

The equipotential lines (ϕ_1) outside the particle [Figs. 6(a)–6(c)] for different values particle-to-electrolyte permittivity ratio shows that the strong surface conduction tends to contract the field lines around the particle. Contraction of field lines slows down the electrophoretic velocity of the dielectric particle.

Figure 7 presents the scaled electrophoretic velocity as a function of the Debye length at a fixed value of the surface charge density. We present results for different values of the dielectric permittivity ratio. It is evident from Fig. 7 that the effect of solid polarization is strong when κa is $O(1)$. The velocity is presented as a function of κa for a fixed value of $\sigma\kappa a$ so as to have a constant surface charge density when Debye length is varied. Our computed results show that the solid polarization effect is negligible for large κa (thin Debye layer) under an electric field $E_0 \ll \kappa\phi_0$. However, it is evident from Fig. 2(c) that the impact of solid polarization for a thin Debye layer is not negligible when the applied electric field and permittivity ratio is large.

The balance of electrical and hydrodynamical forces experienced by the particle in electrophoresis is illustrated in Fig. 8(a). Figures 2(b), 2(c), and 8(a) show that the electrophoretic velocity and forces vary nonlinearly with the imposed electric field. Figure 8(b) shows that the ratio of the electrophoretic velocity between the polarizable particle and the nonpolarizable particle is less than one and it reduces as the electric field is raised. Effect of the particle polarization becomes strong as the imposed field grows. The induced charge electroosmotic flow around the particle produces the hindrance effect and it grows at the quadratic order of the imposed field.

Dependence of the electrophoretic velocity on the dielectric permittivity ratio for different values of the Debye length ($\kappa a = 1, 5, 50$) is illustrated in Figs. 9 and 10. In Figs. 9(a)–9(c) we present the variation for different values of the scaled surface charge density σ of the particle. The dependence of the electrophoretic velocity on the permittivity ratio for different values of the applied electric field when the scaled surface charge density $\sigma = 1.04$ is illustrated in Figs. 10(a)–10(c). Comparison of the electrophoretic velocity of a polarizable particle with the corresponding nonpolarizable particle is also illustrated in those figures. These results indicate that the variation in velocity due to the variation of dielectric permittivity ratio occurs at a faster rate for moderate range of permittivity ratio and this variation with ε_r is higher when κa is $O(1)$. Velocity decays with the increase of permittivity ratio and approaches a constant value when the permittivity ratio becomes large. This saturation in electrophoretic velocity is expected as the particle behaves like a conductor at large values of the permittivity. As far as we know, no theoretical analysis exists for a conducting particle at finite Debye length and nonweak electric field, as considered here. It is evident from the results that U_E for a polarizable particle deviates by a large extent from the corresponding value due to a nonpolarizable particle. Figures 9 and 10 show that a larger imposed electric field (or surface charge density) produces a stronger polarization effect. Figure 10(c) shows that the solid polarization effect for a thin Debye layer is not negligible when the imposed field is strong. It is evident from Figs. 9 and 10 that the difference in electrophoretic velocity of a polarizable particle from the corresponding nonpolarizable particle is highest when $\kappa a = 1$.

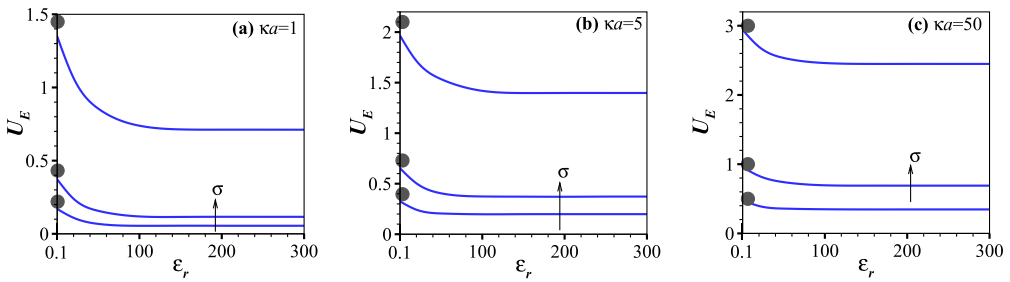

FIG. 9. (Color online) Variation of electrophoretic velocity with ε_r for different σ(=0.5, 1.04, 4.26) when $\beta = 1$ for κa =1, 5, and 50. Here symbols represents the electrophoretic velocity corresponding to a nonpolarizable particle.

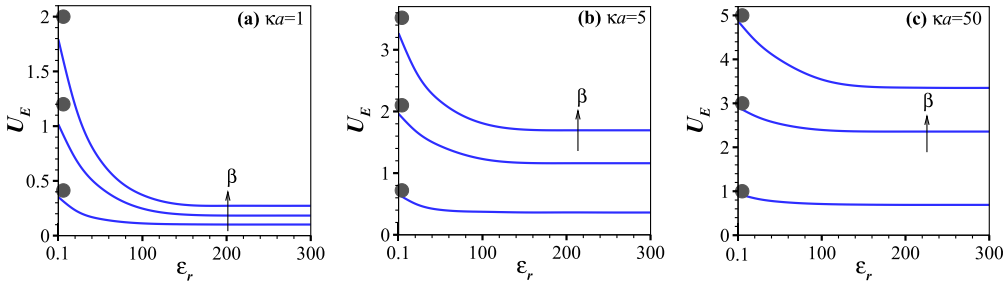

FIG. 10. (Color online) Variation of electrophoretic velocity with the particle-to-electrolyte permittivity ratio at different values of the applied electric field $\beta(=1, 3, 5)$ when $\sigma = 1.04$ for κa =1, 5, and 50. Here symbols represents the electrophoretic velocity corresponding to a nonpolarizable particle.

The variation of the electrophoretic velocity of a polarizable particle with the square of the imposed field for different values of the Debye layer thickness is presented in Fig. 11(a). Results show that the dependence of U_E with β^2, where $\beta = E_0 a/\phi_0$, is similar for all three values of κa considered. At a fixed value of the electric field and Debye length, the electrophoretic velocity increases with the increase of scaled surface charge density. The nonlinear dependence of the electrophoretic velocity with the imposed field is evident from Fig. 11(a). The corresponding variation for a nonpolarizable ($\varepsilon_r = 0$) particle is shown in Fig. 11(b) to analyze quantitatively the variation of electrophoretic velocity with nonweak applied electric field of a nonpolarizable particle. In Fig. 11(b) the variation of the electrophoretic velocity of a nonpolarizable particle with the electric field at different values of the Debye length is shown. A comparison with the velocity obtained by Henry's [24] formula is also made in Fig. 11(b). It may be noted that the electrophoretic velocity of a nonpolarizable particle based on Henry's formula does not take into account the DLP and ion convection effects. As is expected, the results based on Henry's formula overestimate our computed solutions. A linear variation of the electrophoretic velocity for low values of the electric field is evident from the results. At higher values of the imposed field the DLP effect becomes stronger and the dependence of the electrophoretic velocity with the applied electric field is no longer linear even for the nonpolarizable particle.

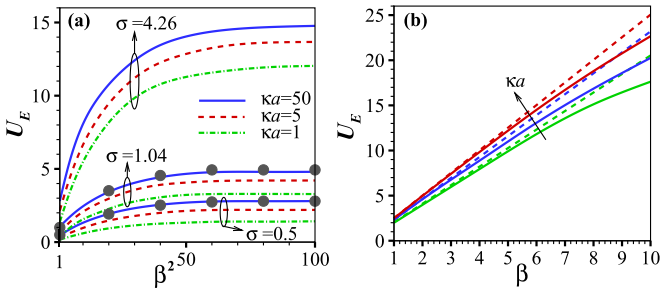

FIG. 11. (Color online) Variation of the electrophoretic velocity U_E of a (a) dielectric particle with β^2 for different $\sigma(=0.5, 1.04, 4.26)$ and $\kappa a(=1, 5, 50)$ when $\varepsilon_r = 50$. Symbols represent the results due to Yariv and Davis [15] for $\zeta = 0.5$ and 1; (b) of nonpolarizable ($\varepsilon_r = 0$) particle with β for different values of $\kappa a(=1, 5, 10)$ when $\zeta = 3$. In Fig. 11(b) the dashed lines represent the Henry velocity.

V. CONCLUSIONS

The electrophoresis of a charged dielectric particle for moderate values of the imposed electric field and finite values of the Debye layer thickness is considered. Results are obtained for a wide range of particle-to-electrolyte dielectric permittivity ratio. A quantitative measure of the electrophoretic velocity based on the force balance is made. None of the previous studies have provided the electrophoretic velocity based on a full nonlinear model. An analytical treatment forbids the investigation of cases with finite Debye length and nonweak electric field. Our computed solution agrees well with the existing asymptotic analysis. The main findings of this study can be highlighted as follows:

(1) Electrophoretic velocity reduces as the particle-to-electrolyte dielectric permittivity ratio is increased and the velocity attains a saturation at large values of the permittivity ratio. This reduction in electrophoretic velocity occurs at a faster rate for a moderate range of the dielectric ratio. The electrophoretic velocity does not vary linearly with the applied electric field when a moderate range of the imposed electric field is considered. The solid polarization gets stronger with the rise of the applied electric field as well as surface charge density of the particle.

(2) The dependence of the electrophoretic velocity on the particle-to-electrolyte dielectric permittivity of the particle is not uniform for any choice of the Debye layer thickness. Variation in electrophoretic velocity due to the variation of the dielectric permittivity ratio occurs at a faster rate when the Debye length is in the order of the particle size. Our computed solution for thin Debye layer case, as has been established in previous studies, i.e., Schnitzer and Yariv [3], shows that the solid polarization is important for higher values of applied electric field and dielectric ratio.

(3) The surface potential strongly depends on the dielectric permittivity ratio when a moderate range of the dielectric permittivity ratio is considered. The surface potential for high values of the Debye-Huckel parameter and permittivity ratio of a dielectric particle approaches to the ζ potential of a conducting particle obtained by the slip-flow model.

ACKNOWLEDGMENT

One of the authors (S.B.) thanks the Department of Science & Technology, Government of India, for providing the financial support through the project under Grant No. SR/S4/MS:740/12.

[1] R. W. O'Brien and L. R. White, J. Chem. Soc. Faraday Trans. **74**, 1607 (1978).
[2] G. Yossifon, I. Frankel, and T. Miloh, Phys. Fluids **19**, 068105 (2007).
[3] O. Schnitzer and E. Yariv, Phys. Fluids **24**, 082005 (2012).
[4] C. Canpolat, S. Qian, and A. Beskok, Microfluid. Nanofluid. **14**, 153 (2013).
[5] T. M. Squires and M. Z. Bazant, J. Fluid Mech. **509**, 217 (2004).
[6] E. Yariv, Phys. Fluids **17**, 051702 (2005).
[7] T. M. Squires and M. Z. Bazant, J. Fluid Mech. **560**, 65 (2006).
[8] H. Zhao and H. H. Bau, Langmuir **23**, 4053 (2007).
[9] E. Yariv, Proc. R. Soc. A **465**, 709 (2009).
[10] M. Abu Hamed and E. Yariv, Proc. R. Soc. A **465**, 1939 (2009).
[11] E. Yariv and T. Miloh, J. Fluid Mech. **595**, 163 (2008).
[12] M. Abu Hamed and E. Yariv, J. Fluid Mech. **627**, 341 (2009).
[13] S. M. Davidson, M. B. Andersen, and A. Mani, Phys. Rev. Lett. **112**, 128302 (2014).
[14] O. Schnitzer and E. Yariv, Phys. Rev. E **89**, 043005 (2014).
[15] E. Yariv and A. M. J. Davis, Phys. Fluids **22**, 052006 (2010).
[16] B. Figliuzzi, W. H. R. Chan, J. L. Moran, and C. R. Buie, Phys. Fluids **26**, 102002 (2014).
[17] O. Schnitzer and E. Yariv, Phys. Rev. E **86**, 021503 (2012).
[18] R. W. O'Brien, J. Colloid Interface Sci. **92**, 204 (1983).
[19] R. W. O'Brien and R. J. Hunter, Can. J. Chem. **59**, 1878 (1981).
[20] O. Schnitzer, R. Zeyde, I. Yavneh, and E. Yariv, Phys. Fluids **25**, 052004 (2013).
[21] O. Schnitzer and E. Yariv, Phys. Fluids **26**, 122002 (2014).
[22] D. A. Saville, Annu. Rev. Fluid Mech. **9**, 321 (1977).
[23] A. S. Khair and T. M. Squires, Phys. Fluids **20**, 087102 (2008).
[24] R. J. Hunter, *Foundations of Colloid Science* (Oxford University Press, New York, 2001).
[25] S. Tseng, P.-H. Yeh, and J.-P. Hsu, Langmuir **30**, 8177 (2014).